ACS APPLIED MATERIALS & INTERFACES

Research Article

www.acsami.org

Highly Stable and Tunable n-Type Graphene Field-Effect Transistors with Poly(vinyl alcohol) Films

Sungjin Kim,[†] Pei Zhao,[§] Shinya Aikawa,[‡] Erik Einarsson,[⊥] Shohei Chiashi,[†] and Shigeo Maruyama*[,†,#]

[†]Department of Mechanical Engineering, The University of Tokyo, 7-3-1 Hongo, Bunkyo-ku, Tokyo 113-8656, Japan

[§]Institute of Applied Mechanics, Zhejiang University, Hangzhou, Zhejiang 310027, China

[‡]Research Institute for Science and Technology, Kougakuin University, 2665-1 Nakano, Hachioji, Tokyo 192-0015, Japan

[⊥]Department of Electrical Engineering, University at Buffalo, The State University of New York, Buffalo, New York 14260, United States

[#]Energy NanoEngineering Laboratory, National Institute of Advanced Industrial Science and Technology (AIST), 1-2-1 Namiki, Tsukuba, 305-8564, Japan

Supporting Information

ABSTRACT: The intrinsic p-type behavior of graphene field-effect transistors (FETs) under ambient conditions poses a fundamental challenge for the assembly of complex electronic devices, such as integrated circuits. In this work, we present a protocol for tunable n-type doping of graphene FETs via poly(vinyl alcohol) (PVA) coating. Using graphene grown by alcohol catalytic chemical vapor deposition, functionalization of the surface by this hydroxyl anion-rich polymer results in an evolution of the FETs from p-type to ambipolar or n-type even under ambient air conditions. The doping level of graphene is strongly related to the PVA film coating parameters, such as solution concentration, hardening temperature, and hardening time. This PVA coating proves to be a simple and stable approach to tuning the Dirac point and doping level of graphene, which is highly desirable and of great significance for the future of graphene-based electronic devices.

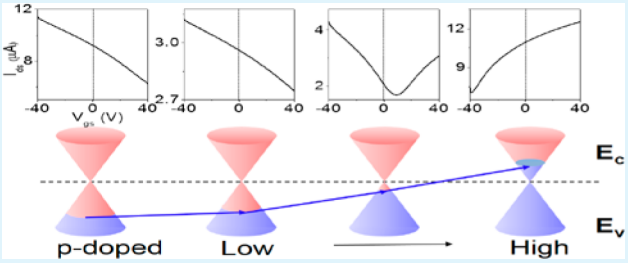

KEYWORDS: *chemical vapor deposition, graphene, n-type doping, field-effect transistor, poly(vinyl alcohol) thin film*

INTRODUCTION

There are many advantages to using graphene for electronic and optoelectronic devices due to graphene's outstanding electrical, mechanical, and optical transparent properties.[1−3] Its many physical and electrical properties, such as its extraordinarily high carrier mobility (up to 200,000 $cm^2\ V^{-1}\ s^{-1}$),[4] ballistic transport distance up to 1 μm,[5] half-integer quantum Hall effect,[6,7] and superior mechanical elasticity,[8] confer its promising candidacy to substitute for silicon in the next generation of electronics. However, the full potential of graphene in the device industry is still restricted by several challenges. For example, it is crucial to open a bandgap in graphene to realize the ON- and OFF-states in electronic devices. Solutions to this challenge involve tailored nanoribbon structures,[9−12] bilayer graphene in the presence of a vertical electric field,[13−16] graphene nanomeshes,[17] and so forth. Furthermore, on the basis of the fact that ambient conditions makes graphene behave as a p-type semimetal,[18] we must adjust the positive and negative carrier concentrations by shifting the Fermi level away from its Dirac point so that the device can also behave as n-type and be assembled into circuits.[19,20] Several approaches to locally change the carrier density have been explored using different dopants, such as gases, alkali metals, polymers, heteroatom, photochemical, and so on.[18,20−26] However, these approaches show disadvantages in device fabrication, such as difficulty in processing or patterning, or poor device stability, applicability, controllability, and so forth. For instance, potassium doping has led to the fabrication of n-type graphene field-effect transistors (FETs) and enabled the integration of more complex devices, such as intragraphene p−n junctions with different device functions.[27] Furthermore, such alkali dopants suffer from immediate degradation upon exposure to air, making them inapplicable for n-type doping of graphene in practical device applications.

In this work, we present a protocol for tunable n-type doping of graphene by functionalizing the surface with a poly(vinyl alcohol) (PVA) film. Using high-quality graphene grown by alcohol catalytic chemical vapor deposition (ACCVD), functionalization of the graphene surface by this hydroxyl anion-rich polymer results in an evolution of the FETs from p-type to ambipolar or n-type. The doping level of graphene is strongly correlated with different treatment conditions of the PVA film, such as the polymer concentration for instance. This PVA coating proves to be a simple and stable approach to

Received: February 14, 2015
Accepted: April 15, 2015
Published: April 15, 2015

DOI: 10.1021/acsami.5b01474
ACS Appl. Mater. Interfaces 2015, 7, 9702−9708

tuning the Dirac point and doping level of graphene, and this environmentally free n-type doping enables us to fabricate more complex electronic devices such as p−n junction diodes, complementary inverters, and numerous complicated logic circuits.

EXPERIMENTAL METHODS

The graphene used in our study was produced by ACCVD using a copper foil enclosure, as described in our previous work.[28] Briefly, the copper substrate was first cleaned by hydrogen chloride, acetone, and isopropanol sequentially to remove the foil protection layer. To smooth the metal surface and remove metal oxides, we annealed the copper substrate at 1000 °C for 20 min in Ar/H_2 (3% H_2). The graphene growth was at 1000 °C with 10 sccm ethanol flow diluted by 300 sccm Ar/H_2, and the growth time was 10 min.[28] Uniform monolayer graphene was obtained on the inside surface of the copper enclosure. For device fabrication, source/drain electrodes were first patterned on a SiO_2/Si (600 nm) substrate using a standard photolithography process. The 40 nm/2 nm thick Pt/Ti electrodes were deposited under high vacuum conditions using a thermal evaporator (ULVAC, VPC-260F) with a quartz crystal thickness meter (ULVAC, CRTM-6000). As-grown graphene was then transferred using 4% poly(methyl methacrylate) (PMMA) (average molecular weight ∼950k, Sigma-Aldrich) in anisole onto the substrate with predefined electrodes, similar to the process reported previously.[29] The PMMA layer was then removed by acetone, followed by annealing the device at 350 °C for 3 h under vacuum conditions. Subsequently, the second photolithography step was adopted to remove the graphene film exclusive of the channel region between the source and drain by exposing to substrate oxygen plasma (100 W, 100 Pa) for ∼1 min.

The PVA solution was prepared by dissolving 1, 10, or 20 wt % PVA powder (average molecular weight ∼1500, Wako) in distilled water. The polymer thin films were formed on the graphene channel by spin-coating the solution at 2000 rpm for 60 s followed by baking at 60−150 °C for 10−30 min.

After the fabrication of pristine and polymer-coated graphene FETs, the devices were characterized using a semiconductor parameter analyzer system (Agilent 4156C) under air and vacuum conditions, scanning electron microscopy (SEM, Hitachi, S-4800, acceleration voltage of 5 kV), and micro-Raman spectroscopy (Nanophoton Raman-11 system, Renishaw inVia system).

RESULTS AND DISCUSSION

Figure 1a presents an SEM image of as-grown graphene on the inside surface of a copper enclosure. The graphene film shows uniform high quality, as demonstrated by the scanning Raman map in Figure 1b. The number of active graphene layers was determined from the intensity ratio between the Raman G′- and G-bands ($I_{G'}/I_G$), which exhibits an average value of ∼2. Only a small disorder band is visible in the Raman spectra (see Figure S1 in the Supporting Information), which proves the high quality monolayer of graphene. Its full width at half-maximum (FWHM) was 32−35 cm^{-1} in our as-grown graphene, consistent with the value reported for monolayer graphene.[30] Panels c and d in Figure 1 illustrate the schematic and SEM image of our graphene FETs on silicon substrate with a bottom gate and a coated polymer film as dopants. To date, PVA was an encouraging material as polymer dielectrics in flexible devices or alignment layer in liquid crystal applications due to its high dielectric constant, good surface alignment effect, photosensitivity, and good resistance to damage by solvents involved in the lift-off process.[31,32] We have examined the doping effect of the graphene devices with PVA coating by preparing as-grown graphene on a SiO_2/Si substrate and measuring its gate response to different polymer film

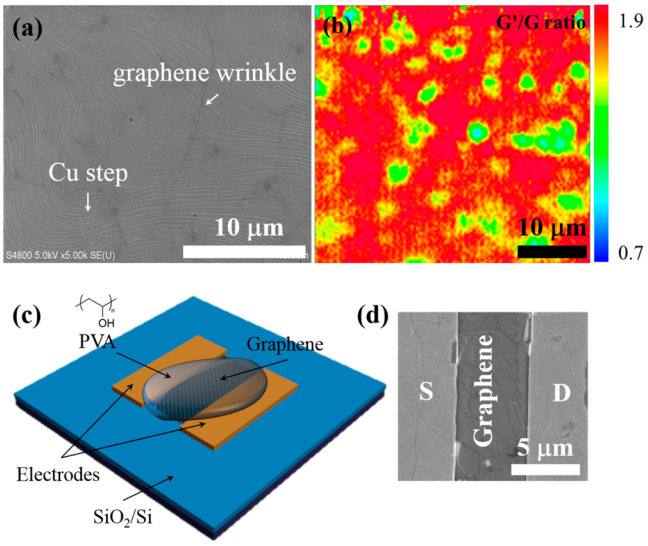

Figure 1. (a) SEM image of as-grown graphene on a copper substrate grown via ACCVD. (b) Intensity ratio of G′- to G-band of scanning Raman spectroscopy using an excitation energy of 514.5 nm (2.41 eV). (c) Schematic illustration of polymer-film-coated graphene field-effect transistors with source, drain, and gate electrodes. (d) Corresponding SEM image of graphene transferred onto a SiO_2/Si substrate (600 nm thick oxide layer) between the source/drain electrodes (channel length = 5 μm, width = 20 μm).

conditions, such as annealing time, temperature, and polymer concentration. The functionalization of the graphene surface by hydroxyl anion-rich polymers leads to the development of graphene from p-type to n-type or ambipolar. Here, doping by functional groups of adsorbed polymers on graphene presents a simple means by which to change the doping level. Furthermore, we achieve n-type graphene FETs that are stable under air without keeping the graphene in a vacuum or an inert environment, which is discussed in more detail below.

We demonstrate that the adsorption of PVA on graphene results in a negative shift of the Dirac point. Similar phenomena were also reported for single-walled carbon nanotube FETs and graphene using poly(ethylene imine) (PEI) from other groups.[23,33,34] This is illustrated in Figure 2a, where the transfer curve ($I_{ds}-V_{gs}$) after PVA exposure exhibits a shift of the neutrality point to more negative gate voltages under ambient conditions. In Figure 2a, our as-transferred graphene FETs show p-type transport behavior with highly positive Dirac points of >40 V. The neutrality point of the as-grown graphene device was beyond the gate voltage range, for instance, from −100 to 100 V, because the as-grown graphene was heavily p-type doped, as shown in Figure S2 in the Supporting Information. This is because the adsorption of water molecules or/and oxygen can affect the electrical properties of graphene.[22] The intrinsic Fermi level of graphene is downshifted to the valence band when graphene is exposed readily to ambient air. Initially, the Dirac point of the graphene transistors is shifted ∼5 V after as-coated graphene devices, and the Dirac voltage was then shifted considerably to negative voltages, indicating an n-type doping effect of coating with a PVA film on monolayer graphene. The current level was reduced with ambipolar behavior. The Dirac point of the doped graphene transistors was shifted significantly from >40 V to approximately −20 V after 7 days. A 10 wt % doped graphene device was left under ambient conditions for one month, and its Dirac voltage moved

DOI: 10.1021/acsami.5b01474
ACS Appl. Mater. Interfaces 2015, 7, 9702−9708

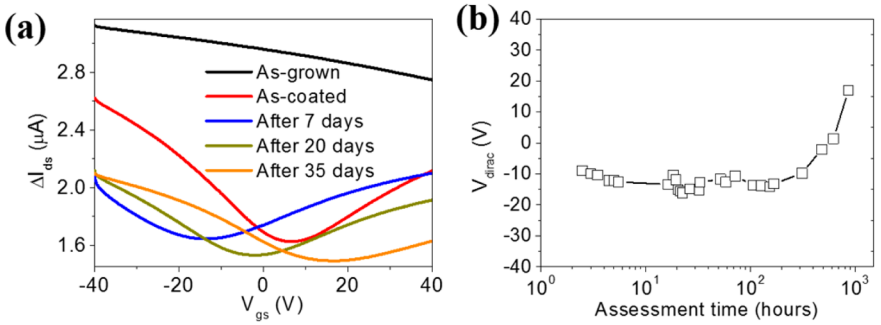

Figure 2. Corresponding electronic transport properties of 10 wt % PVA-treated graphene devices. (a) Stability of transfer characteristics of 10 wt % PVA graphene devices as a function of time evaluated under ambient conditions (channel length = 20 μm, width = 10 μm, V_{ds} = −10 mV). (b) Dirac point shift of the 10 wt % PVA-coated graphene transistors in terms of assessment time under ambient conditions.

to positive gate voltage, but the n-type doping behavior was still preserved, as shown in Figure 2a. The air stability of a PVA-doped graphene transistor was monitored by measuring the performance as a function of time, in which graphene was doped with a solution concentration of 10 wt % PVA and monitored for more than 30 days, as shown in Figure 2b. After more than 30 days, the Dirac point of these graphene devices kept in ambient air was not shifted to over 0 V and exhibited ambipolar behavior, indicating that doping with PVA was still effective in air to donate electrons to the unintentional p-doping of graphene and to recover its expected ambipolar behavior for pristine graphene. The doping-induced electric transport asymmetry shown in Figure 2a is caused by a combination of the neutrality point misalignment at the electrode/channel interface and the variable density of states of the graphene electrodes.[34]

We find that hardening temperature is another factor that can affect the electron transport behavior of graphene FETs using 10 wt % PVA solution. As shown in Figure 3a, similar heavily p-type unipolar to ambipolar conversions were observed when using different baking temperatures. The Dirac point of a graphene device changes as temperature increases, for instance, the corresponding transfer curves (I_{ds}−V_{gs}) of graphene FETs are gradually shifted from 24 V when hardened at 80 °C to −7 V when hardened at 150 °C. Panels b and c from Figure 3 show the Dirac point shift as a function of temperature with a standard deviation and resistance of graphene from source-drain current modulation with various temperatures, respectively. We can also tune the Fermi level of the graphene in a straightforward manner using coated PVA films with different hardening times, as shown in Supporting Information Figure S3a−f. The Dirac point of PVA-doped graphene transistors initially induced a down-shift compared to that of the as-grown graphene, and then saturated as the baking time increased. Our results show that the hardening temperature and time can control the Dirac point of graphene devices. Figures S3a−f in the Supporting Information depict devices with or without coating polymer films on graphene, which show the I_{ds}−V_{ds} characteristics that can be interpreted as doped graphene. The transfer characteristics of GFETs were linear before doping. In the case of 10 wt % PVA, the total resistance, including contact and channel, increases to 4.6 kΩ from 1.9 kΩ due to the reduction of carrier concentration in PVA-doped graphene devices as in Figure S4a in the Supporting Information. A shift in the Fermi level owing to charge transfer significantly affects carrier density in graphene.

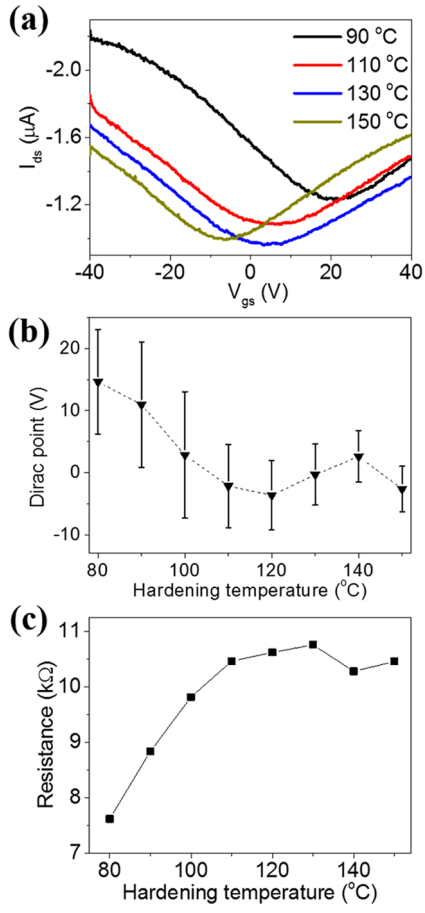

Figure 3. Electronic properties of PVA-doped graphene transistors (channel length = 10 μm, width = 10 μm). (a) Corresponding I_{ds}−V_{gs} characteristics of 10 wt % PVA-coated graphene devices as a function of different hardening temperatures for 10 min. (b) Dirac point position shift of graphene transistors depends on diverse hardening temperatures with standard deviation. (c) Resistance of graphene depends on different hardening temperatures.

To estimate the ability of PVA to donate electrons to graphene, we compared the Dirac point shifts between graphene devices based on PVA solutions with different concentrations. Because PVA consists of anion-rich groups, which presumably bear a lone pair of electrons, we considered anion molecules adsorbed on graphene. Electron carriers from these sites are pulled into the graphene monolayer by the downward electric field induced by a back-gate voltage,

DOI: 10.1021/acsami.5b01474
ACS Appl. Mater. Interfaces 2015, 7, 9702−9708

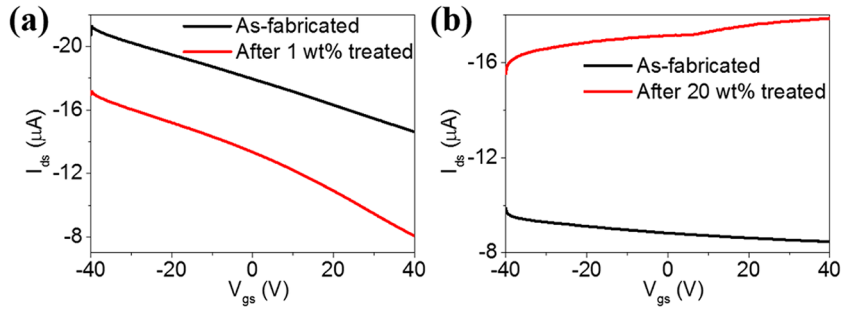

Figure 4. Comparisons of electronic properties between high concentration (20 wt %) PVA-treated CVD graphene transistors and low concentration (1 wt %) PVA-treated devices. (a) Corresponding transfer (I_{ds}–V_{gs}) characteristics of as-grown and low concentration solution of PVA-doped graphene devices as a function of gate voltage before and after doping, respectively. (b) Corresponding transfer curves of as-grown and high concentration solution (20 wt %) of PVA-doped graphene transistors as a function of gate voltage before and after doping, respectively.

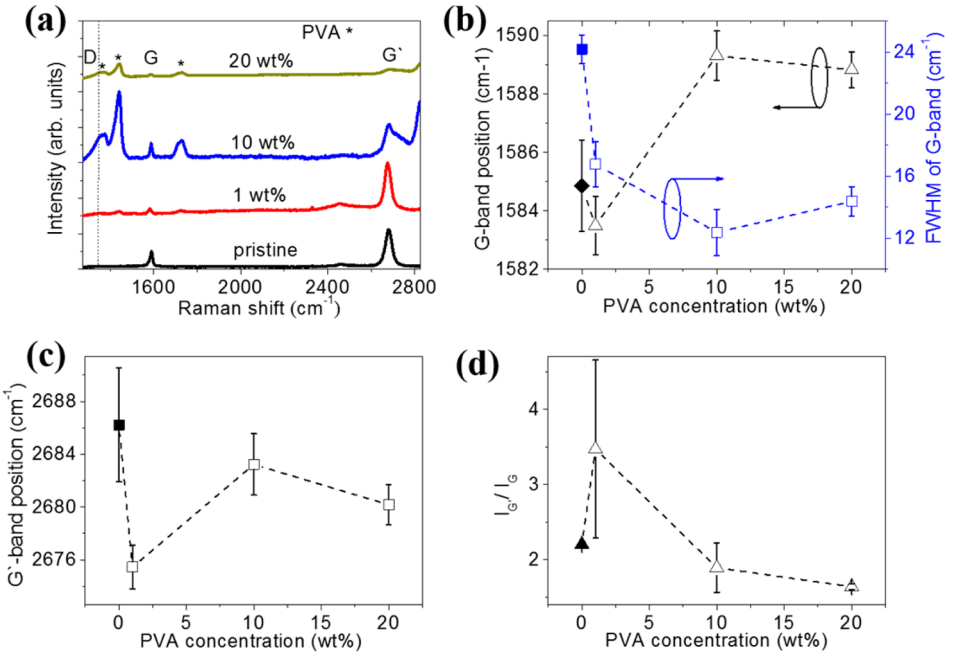

Figure 5. (a) Raman spectra of monolayer graphene doped with various concentration solutions of PVA on a SiO_2/Si substrate. The intensity of the G′- to G-band ratio of as-grown graphene was >2, and the peak position of G- and G′-bands are approximately 1585 and 2688 cm^{-1}. Asterisks indicate the Raman features from the PVA films. (b) G-band position shift and its FWHM in terms of PVA concentration. (c) G′-band position shift of monolayer graphene as a function of PVA concentrations. (d) Intensity of G′- to G-band ratio as a function of various concentration solutions of PVA.

resulting in a sudden increase in electron density and hence increased conductance. Prior to PVA coating, we first confirmed the transfer characteristics and Raman spectroscopy of all as-grown graphene were the appropriate quality and doping level. As an extension of PVA concentration, the neutrality point of the graphene device is readily shifted to a negative gate voltage (i.e., n-type electrical switching behavior) because of electron transfer to graphene from coated polymer films. The I_{ds}–V_{gs} curves from low concentration solutions (1 wt %) of PVA-doped graphene devices does not significantly change when compared to that of pristine graphene transistors as shown in Figure 4a. This may be the reason that the p-type carrier is compensated by light n-doping, resulting in the reduction of drain current observed in Figure 4a. On the other hand, there was no appreciable n-dopant remaining at the low concentration of 1 wt %. This will be discussed in more detail later. The transfer characteristics of high concentration solutions (20 wt %) of PVA-coated graphene devices converted to n-type from p-type behaviors is shown in Figure 4b.

To confirm the n-type doping effect of PVA on as-grown graphene films and to derive a better understanding of interfacial electron transfer, we obtained Raman spectra from these graphene FETs. We characterized both the as-transferred and doped graphene films with different concentration solutions of PVA and compared their Raman spectra features. The G-band and G′-band positions of as-grown graphene are ~1584 cm^{-1} and ~2688 cm^{-1}, respectively.[35] Previous reports for in situ Raman measurements using gate tuning of Dirac points found that the G-band position of graphene upshifts for both n-type and p-type doping.[36,37] On the other hand, the G′-band downshifts with heavy electron donation, and the G′- to G-band intensity ratio is strongly dependent on the doping level. As for our graphene devices, the as-grown graphene shows a slight upshift of the G-band position due to unintentional p-type doping by oxygen and other impurities

DOI: 10.1021/acsami.5b01474
ACS Appl. Mater. Interfaces 2015, 7, 9702–9708

during the transfer process (Figure 5a and b). After doping with a low concentration solution of PVA, the graphene G-band starts to downshift to lower wavenumbers, indicating a doping effect that is consistent with the observed conversion from p-type to ambipolar behavior. As the PVA concentration increases, the G-band position upshifts as the graphene FET becomes n-type, which was also observed for doping by gate tuning. The evolution of the G-band FWHM is opposite to that of the G-band position, which exhibits a narrowing for both electron and hole doping. Furthermore, the change in the G′-band position is smaller than that in G-band position, as shown in Figure 5c. Another important parameter to estimate the doping level is the intensity ratio of G′ to G-band. $I_{G'}$ to I_G exhibits a strong dependence on the PVA doping concentration, as shown in Figure 5d. As the PVA concentration increased, PVA peaks were clearly observed at 1362 and 1441 cm^{-1}.[38] The transfer characteristics of as-grown graphene and typical PVA-coated graphene devices are shown in Supporting Information Figures S4b and c, with higher hole and electron mobilities of ~1116 $cm^2\ V^{-1}\ s^{-1}$ and ~850 $cm^2\ V^{-1}\ s^{-1}$, respectively, compared to as-grown graphene FETs (hole mobility of ~397 $cm^2\ V^{-1}\ s^{-1}$) calculated from the transfer curves (I_{ds}–V_{gs}). The field-effect mobilities of electrons and holes were derived from the slope of the source-drain current variation from gate voltage to the linear regime using the equation $\mu = (L_c/(WCV_d))(\Delta I_{ds}/\Delta V_{gs})$, where L_c and W are the channel length and width, $\Delta I_{ds}/\Delta V_{gs}$ is the transconductance, C is the gate capacitance, and V_d is the source-drain voltage. The hole mobility for 10 wt % PVA-coated graphene devices (2200 $cm^2\ V^{-1}\ s^{-1}$) showed ~2× that of the pristine FET (1260 $cm^2\ V^{-1}\ s^{-1}$). It has been reported that n-type doping on graphene by the amine groups improves or recovers the electrical properties of graphene.[39,40] The anion in the PVA film similarly donates its lone pair electron to graphene, which increases the electron carrier density and induces n-type doping. The charge compensates the p-type doping to recover the intrinsic electrical properties of the as-grown graphene and induces improved charge carrier mobility. Both type conversion and the changed mobilities are reproducible in many graphene FETs that were independently prepared, as shown in Figure S5a and b in the Supporting Information. The V_{gs} dependent carrier density n calculated from the intrinsic mobility of CVD graphene is shown in Figure S5c in the Supporting Information. The intrinsic mobility of graphene FETs was derived from $\mu_i = 1/n_i e\rho_{xx}$. In the case of PVA-doped graphene FET, the carrier concentration was derived from $n_{PVA} = \sigma/e\mu_i$. We can determine the carrier concentration of both n- and p-type as the above step. Figure S5d in the Supporting Information shows an optical micrograph of graphene FETs fabricated by e-beam lithography.

Electronic properties of graphene can be adjusted by chemical modifications.[22] However, one drawback of chemical doping is the return of an n-type FET to p-type when exposed to air, because the dopants are readily oxidized and lose their ability for n-type doping. For instance, graphene FETs doped with inorganic (NO_2)[41] and organic molecules (amines)[34] exhibit n-type behavior in a vacuum but readily change to p-type behavior upon exposure to air. PEI, which contains an amine group, leads to doped graphene FETs that exhibit n-type behavior with a relatively high on/off ratio but also changes back to p-type under ambient conditions. The 10 wt % PVA-coated graphene FETs result in n-type characteristics that are stable under ambient air conditions for one month, as shown in Figure 2a and b. To assess device stability, we doped graphene FETs with medium (10 wt %) and high (20 wt %) concentration solutions of PVA, and then left the devices under ambient conditions for up to three months. The device doped with 10 wt % PVA solution returned to p-type characteristics (similar to the as-grown graphene device), as shown in Figure 6a. However, after heat treatment of the

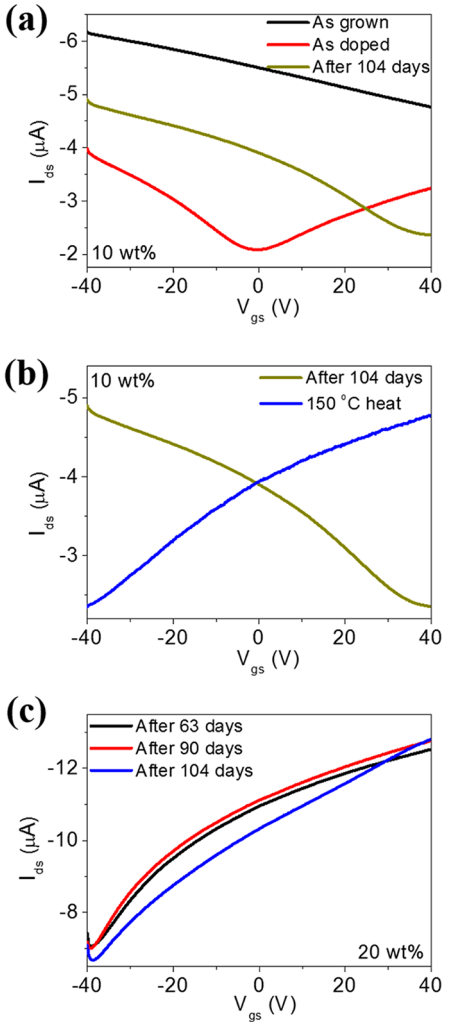

Figure 6. Long-term stability of n-type doping. (a) Corresponding I_{ds}–V_{gs} characteristics of as-grown, as-doped (10 wt %), and after 104 days of graphene transistors under ambient air conditions. (b) Corresponding I_{ds}–V_{gs} characteristics of lightly doped (10 wt %) graphene devices after 104 days and after reheat treatment at 150 °C. (c) Stability of I_{ds}–V_{gs} characteristics of 20 wt % PVA-doped graphene device after 63, 90, and 104 days.

sample at 150 °C for 30 min, the device fully recovered the n-type behavior (Figure 6b). This remarkable reversibility can be attributed to charge transfer as well as the passivation layer by the PVA film, which prevents ambient gases from being adsorbed onto the graphene surface. Although water molecules are adsorbed into the PVA films as time passes, these molecules can be removed by heat treatment. In Figure 6c, the corresponding I_{ds}–V_{gs} characteristics of a device doped with 20 wt % PVA were slightly reduced, but n-type doping behavior was maintained under ambient conditions for up to three months. This high stability in PVA allows for the fabrication of circuits using conventional lithography under ambient con-

DOI: 10.1021/acsami.5b01474
ACS Appl. Mater. Interfaces 2015, 7, 9702–9708

ditions. It is expected that this reversible stability will prove beneficial in many aspects of device fabrication in the future.

CONCLUSION

In summary, we demonstrate a method for implementing n-type doping of as-grown graphene in ambient conditions using a solution-based PVA coating. Varying the temperature and hardening time of PVA coated on graphene films can affect the extent of the n-type doping level. Furthermore, the graphene FETs can be converted from p-type transport behavior to ambipolar and n-type transport behavior by PVA doping with different concentration solutions. We also demonstrate long-term stability of the n-doped graphene transistors up to three months in ambient conditions. The highly stable n-doping originates from molecular charge transfer doping, and PVA films act as a passivation layer against p-doping from chemical species in the ambient environment. We believe our approach will improve the long-term stability of doped graphene FETs, further enabling us to fabricate basic logic circuits that are stable under ambient conditions.

ASSOCIATED CONTENT

Supporting Information

Raman spectra of as-grown graphene and comparison of as-transferred graphene and doped graphene, including device performance. This material is available free of charge via the Internet at http://pubs.acs.org.

AUTHOR INFORMATION

Corresponding Author

*E-mail: maruyama@photon.t.u-tokyo.ac.jp. Phone: 81-3-5841-6421. Fax: 81-3-5800-6983.

Notes

The authors declare no competing financial interest.

ACKNOWLEDGMENTS

A part of this work was financially supported by Grants-in-Aid for Scientific Research (22226006, 25630063, 25107002, 15H02219) and the IRENA Project by JST-EC DG RTD, Strategic International Collaborative Research Program, SICORP. We also acknowledge support from the Center for Nano Lithography & Analysis (The University of Tokyo) supported by "Nanotechnology Platform" (Project No. 12024046) of MEXT, Japan. A part of this work was also supported by "Global Center for Excellence for Mechanical Systems Innovation" (The University of Tokyo), and VLSI Design and Education Center (VDEC), The University of Tokyo, in collaboration with Cadence Corporation.

REFERENCES

(1) Avouris, Ph.; Chen, Z.; Perebeinos, V. Carbon-Based Electronics. *Nat. Nanotechnol.* **2007**, *2*, 605−615.
(2) Geim, A. K.; Novoselov, K. S. The Rise of Graphene. *Nat. Mater.* **2007**, *6*, 183−191.
(3) Novoselov, K. S.; Fal'ko, V. I.; Colombo, L.; Gellert, P. R.; Schwab, M. G.; Kim, K. A Roadmap for Graphene. *Nature* **2012**, *490*, 192−200.
(4) Morozov, S. V.; Novoselov, K. S.; Katsnelson, M. I.; Schedin, F.; Elias, D. C.; Jaszczak, J. A.; Geim, A. K. Giant Intrinsic Carrier Mobilities in Graphene and Its Bilayer. *Phys. Rev. Lett.* **2008**, *100*, 016602.
(5) Du, X.; Skachko, I.; Barker, A.; Andrei, E. Y. Approaching Ballistic Transport in Suspended Graphene. *Nat. Nanotechnol.* **2008**, *3*, 491−495.
(6) Du, X.; Skachko, I.; Duerr, F.; Luican, A.; Andrei, E. Y. Fractional Quantum Hall Effect and Insulating Phase of Dirac Electrons in Graphene. *Nature* **2009**, *462*, 192−195.
(7) Bolotin, K. I.; Ghahari, F.; Shulman, M. D.; Stormer, H. L.; Kim, P. Observation of The Fractional Quantum Hall Effect in Graphene. *Nature* **2009**, *462*, 196−199.
(8) Lee, C.; Wei, X.; Kysar, J. W.; Hone, J. Measurement of The Elastic Properties and Intrinsic Strength of Monolayer Graphene. *Science* **2008**, *321*, 385−388.
(9) Han, M. Y.; Özyilmaz, B.; Zhang, Y.; Kim, P. Energy Band-Gap Engineering of Graphene Nanoribbons. *Phys. Rev. Lett.* **2007**, *98*, 206805.
(10) Chen, Z.; Lin, Y.-M.; Rooks, M. J.; Avouris, Ph. Graphene Nano-Ribbon Electronics. *Phys. E* **2007**, *40*, 228−232.
(11) Li, X.; Wang, X.; Zhang, L.; Lee, S.; Dai, H. Chemically Derived, Ultrasmooth Graphene Nanoribbon Semiconductors. *Science* **2008**, *319*, 1229−1232.
(12) Wang, X.; Ouyang, Y.; Li, X.; Wang, H.; Guo, J.; Dai, H. Room-Temperature All-Semiconducting Sub-10-nm Graphene Nanoribbon Field-Effect Transistors. *Phys. Rev. Lett.* **2008**, *100*, 206803.
(13) Ohta, T.; Bostwick, A.; Seyller, T.; Horn, K.; Rotenberg, E. Controlling The Electronic Structure of Bilayer Graphene. *Science* **2006**, *313*, 951−954.
(14) Castro, E. V.; Novoselov, K. S.; Morozov, S. V.; Peres, N. M. R.; Lopes dos Santos, J. M. B.; Nilsson, J.; Guinea, F.; Geim, A. K.; Castro Neto, A. H. Biased Bilayer Graphene: Semiconductor with a Gap Tunable by the Electric Field Effect. *Phys. Rev. Lett.* **2007**, *99*, 216802.
(15) Xia, F.; Farmer, D. B.; Lin, Y.-M.; Avouris, Ph. Graphene Field-Effect Transistors with High On/Off Current Ratio and Large Transport Band Gap at Room Temperature. *Nano Lett.* **2010**, *10*, 715−718.
(16) Zhang, Y.; Tang, T.-T.; Girit, C.; Hao, Z.; Martin, M. C.; Zettl, A.; Crommie, M. F.; Ron Shen, Y.; Wang, F. Direct Observation of a Widely Tunable Bandgap in Bilayer Graphene. *Nature* **2009**, *459*, 820−823.
(17) Bai, J.; Zhong, X.; Jiang, S.; Huang, Y.; Duan, X. Graphene Nanomesh. *Nat. Nanotechnol.* **2010**, *5*, 190−194.
(18) Levesque, P. L.; Sabri, S. S.; Aguirre, C. M.; Guillemette, J.; Siaj, M.; Desjardins, P.; Szkopek, T.; Martel, R. Probing Charge Transfer at Surfaces Using Graphene Transistors. *Nano Lett.* **2011**, *11*, 132−137.
(19) Castro Neto, A. H.; Guinea, F.; Peres, N. M. R.; Novoselov, K. S.; Geim, A. K. The Electronic Properties of Graphene. *Rev. Mod. Phys.* **2009**, *81*, 109−162.
(20) Dong, X.; Fu, D.; Fang, W.; Shi, Y.; Chen, P.; Li, L.-J. Doping Single-Layer Graphene with Aromatic Molecules. *Small* **2009**, *5*, 1422−1426.
(21) Guo, B.; Liu, Q.; Chen, E.; Zhu, H.; Fang, L.; Gong, J. R. Controllable N-Doping of Graphene. *Nano Lett.* **2010**, *10*, 4975−4980.
(22) Schedin, F.; Geim, A. K.; Morozov, S. V.; Hill, E. W.; Blake, P.; Katsnelson, M. I.; Novoselov, K. S. Detection of Individual Gas Molecules Adsorbed on Graphene. *Nat. Mater.* **2007**, *6*, 652−655.
(23) Yan, Z.; Yao, J.; Sun, Z.; Zhu, Y.; Tour, J. M. Controlled Ambipolar-to-Unipolar Conversion in Graphene Field-Effect Transistors Through Surface Coating with Poly(ethylene imine)/Poly(ethylene glycol) films. *Small* **2012**, *8*, 59−62.
(24) Li, X.; Tang, T.; Li, M.; He, X. Photochemical Doping of Graphene Oxide Thin Films with Nitrogen for Electrical Conductivity Improvement. *J. Mater. Sci.: Mater. Electron.* **2015**, *26*, 1770−1775.
(25) Wang, X.; Sun, G.; Routh, P.; Kim, D.-H.; Huang, W.; Chen, P. Heteroatom-doped Graphene Materials: Syntheses, Properties and Applications. *Chem. Soc. Rev.* **2014**, *43*, 7067−7098.
(26) Li, X.; Tang, T.; Li, M.; He, X. Nitrogen-doped Graphene Films from Simple Photochemical Doping for n-type Field-Effect Transistors. *Appl. Phys. Lett.* **2015**, *106*, 013110.

DOI: 10.1021/acsami.5b01474
ACS Appl. Mater. Interfaces 2015, 7, 9702−9708

(27) Chen, J.-H.; Jang, C.; Adam, S.; Fuhrer, M. S.; Williams, E. D.; Ishigami, M. Charged-Impurity Scattering in Graphene. *Nat. Phys.* **2008**, *4*, 377−381.
(28) Zhao, P.; Kumamoto, A.; Kim, S.; Chen, X.; Hou, B.; Chiashi, S.; Einarsson, E.; Ikuhara, Y.; Maruyama, S. Self-Limiting Chemical Vapor Deposition Growth of Monolayer Graphene from Ethanol. *J. Phys. Chem. C* **2013**, *117*, 10755−10763.
(29) Li, X.; Cai, W.; An, J.; Kim, S.; Nah, J.; Yang, D.; Piner, R.; Velamakanni, A.; Jung, I.; Tutuc, E.; Banerjee, S. K.; Colombo, L.; Ruoff, R. S. Large-Area Synthesis of High-Quality and Uniform Graphene Films on Copper Foils. *Science* **2009**, *324*, 1312−1314.
(30) Malard, L. M.; Pimenta, M. A.; Dresselhaus, G.; Dresselhaus, M. S. Raman Spectroscopy in Graphene. *Phys. Rep.* **2009**, *473*, 51−87.
(31) Peng, X.; Horowitz, G.; Fichou, D.; Garnier, F. All-Organic Thin-Film Transistors made of Alpha-Sexithienyl Semiconducting and Various Polymeric Insulating Layers. *Appl. Phys. Lett.* **1990**, *57*, 2013−2015.
(32) Swiggers, M. L.; Xia, G.; Slinker, J. D.; Gorodetsky, A. A.; Malliaras, G. G.; Headrick, R. L.; Weslowski, B. T.; Shashidhar, R. N.; Dulcey, C. S. Orientation of Pentacene Films Using Surface Alignment Layers and Its Influence on Thin-Film Transistor Characteristics. *Appl. Phys. Lett.* **2001**, *79*, 1300−1302.
(33) Aikawa, S.; Einarsson, E.; Thurakitseree, T.; Chiashi, S.; Nishikawa, E.; Maruyama, S. Deformable Transparent All-Carbon-Nanotube Transistors. *Appl. Phys. Lett.* **2012**, *100*, 063502.
(34) Farmer, D. B.; Golizadeh-Mojarad, R.; Perebeinos, V.; Lin, Y.-M.; Tulevski, G. S.; Tsang, J. C.; Avouris, Ph. Chemical Doping and Electron-Hole Conduction Asymmetry in Graphene Devices. *Nano Lett.* **2009**, *9*, 388−392.
(35) Ferrari, A. C.; Meyer, J. C.; Scardaci, V.; Casiraghi, C.; Lazzeri, M.; Mauri, F.; Piscanec, S.; Jiang, D.; Novoselov, K. S.; Roth, S.; Geim, A. K. Raman Spectrum of Graphene and Graphene Layers. *Phys. Rev. Lett.* **2006**, *97*, 187401.
(36) Pisana, S.; Lazzeri, M.; Casiraghi, C.; Novoselov, K. S.; Geim, A. K.; Ferrari, A. C.; Mauri, F. Breakdown of The Adiabatic Born-Oppenheimer Approximation in Graphene. *Nat. Mater.* **2007**, *6*, 198−201.
(37) Das, A.; Pisana, S.; Chakraborty, B.; Piscanec, S.; Saha, S. K.; Waghmare, U. V.; Novoselov, K. S.; Krishnamurthy, H. R.; Geim, A. K.; Ferrari, A. C.; Sood, A. K. Monitoring Dopants by Raman Scattering in an Electrochemically Top-gated Graphene Transistor. *Nat. Nanotechnol.* **2008**, *3*, 210−215.
(38) Thomas, P. S.; Stuart, B. H. A Fourier Transform Raman Spectroscopy Study of Water Sorptin by PVA. *Spectrochim. Acta, Part A* **1997**, *53*, 2275−2278.
(39) Yan, Z.; Sun, Z.; Lu, W.; Yao, J.; Zhu, Y.; Tour, J. M. Controlled Modulation of Electronic Properties of Graphene by Self-Assemble Monolayers on SiO_2 Substrates. *ACS Nano* **2011**, *5*, 1535−1540.
(40) Suk, J. W.; Lee, W. H.; Lee, J.; Chou, H.; Piner, R. D.; Hao, Y.; Akinwande, D.; Ruoff, R. S. Enhancement of the Electrical Properties of Graphene Grown by Chemical Vapor Deposition via Controlling the Effects of Polymer Residue. *Nano Lett.* **2013**, *13*, 1462−1467.
(41) Williams, J. R.; Dicarlo, L.; Marcus, C. M. Quantum Hall Effect in a Gate-Controlled p-n Junction of Graphene. *Science* **2007**, *317*, 638−641.

DOI: 10.1021/acsami.5b01474
ACS Appl. Mater. Interfaces 2015, 7, 9702−9708